NUMERICAL STUDY ON SHEAR STRENGTH DEGRADATION AFTER FLEXURAL YIELDING OF RC MEMBER SUBJECTED TO CYCLIC LOADING

H. FURUHASHI[1*†], H. NAKAMURA[2], Y. YAMAMOTO[3]

[1]*Department of Civil Engineering, Nagoya University, Japan*

[2] *Department of Civil Engineering, Nagoya University, Japan*

[3] *Department of Civil Environmental Engineering, National Defense Academy, Japan*

ABSTRACT

In this study, degradation process of shear strength after flexural yielding of RC member subjected to cyclic loading was evaluated numerically, in which 3D Rigid Body Spring Model (3D RBSM) was used. Firstly, shear failure after flexural yielding of RC beam subjected to cyclic loading was simulated and applicability of 3D RBSM was confirmed. Then, a method which can evalute the degradation process of shear strength after flexural yielding was proposed. It was shown that the strength degradation curve obtained by analysis shows similar behavior with the equation obtained by statistical procedure.

Keywords: Shear Failure after Yielding, Shear Strength, Cyclic Loading, 3D RBSM

1. INTRODUCTION

A basic concept of seismic design for RC structures is that shear failure is not permitted to prevent fatal damage with sudden load drop. In design specification, several rules such as arrangement of web reinforcement, ductility evaluation and so on are provided to achieve the concept (JSCE 2012).

It is known that shear failure after flexural yielding occurs under cyclic loading, even when flexural failure occurs under monotonic loading for same member. It is often explained that the reason why the failure mode occurs under cyclic loading is that the shear strength degrades under cyclic loading after flexural yielding according to the displacement increase, although shear strength is higher than flexural strength in the initial stage as shown Figure 1. Based on the explanation, the shear strength degradation curves were proposed by statistical

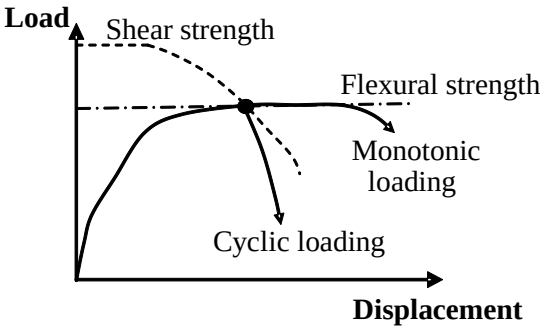

Figure 1: shear failure after flexural yielding

* Corresponding author: Email: furuhashi.hiroki@b.mbox.nagoya-u.ac.jp

† Presenter: Email: furuhashi.hiroki@b.mbox.nagoya-u.ac.jp

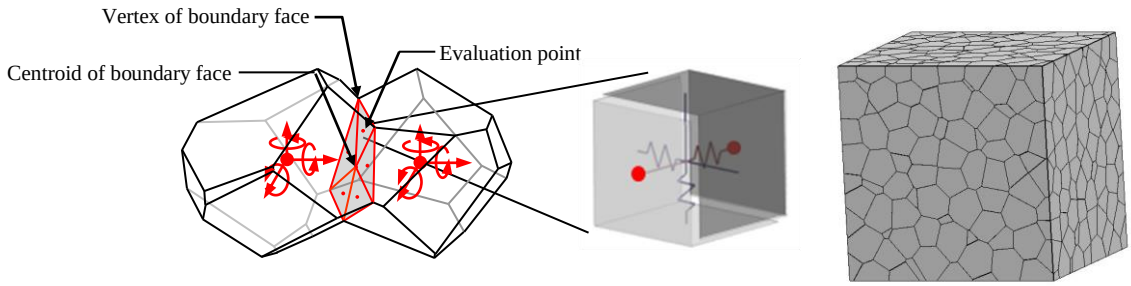

Figure 2: (a) Rigid-body-spring model and (b) Voronoi diagram

procedure using many test results (Priestley et al. 1996; Ohe and Yoshikawa 2002). However, the mechanism of shear failure under cyclic loading has not be clarified, and shear strength degradation has not been evaluated determinately.

In this study, shear failure after flexural yielding of RC beam subjected cyclic loading is simulated in which 3D Rigid Body Spring Model (3D RBSM) with constitutive models under cyclic behavior is used and the applicability of the method is confirmed. Moreover using the method, the degradation process of the shear strength according to the displacement increase was evaluated numerically.

2. NUMERICAL MODEL

2.1. Three-Dimensional Rigid Body Spring Model (3D RBSM)

In RBSM, concrete is modeled as an assemblage of rigid particles interconnected by springs along their boundary surfaces (Figure 2a), which is easy to simulate concrete cracking process and its effects. The crack pattern is strongly affected by the mesh design as the cracks initiate and propagate through the interface boundaries of particles. Therefore, a random geometry of rigid particles is generated by a Voronoi diagram (Figure 2b), which reduces mesh bias on the initiation and propagation of potential cracks.

The response of the spring model provides an insight into the interaction among the particles, which is different from models based on continuum mechanics. In this model, each rigid particle has three translational and three rotational degrees of freedom defined at the nuclei (or nodal points) that define the particles according to the Voronoi diagram (Figure 2a). The boundary surface of two particles is divided into several triangles with a center of gravity and vertices of the surface. One normal and two shear springs are set at the center of each triangle. By distributing the springs in this way, over the Voronoi facet common to two neighboring nodal points, this model accounts for the effects of bending and torsional moment without the need to set any rotational springs (Yasar et al. 2011).

2.2. Concrete Material Model

The constitutive models for tension, compression and shear that are used in 3D RBSM are shown in Figure 3 (Yamamoto et al. 2013). The tensile model for normal springs is shown in Figure 3a. Up to

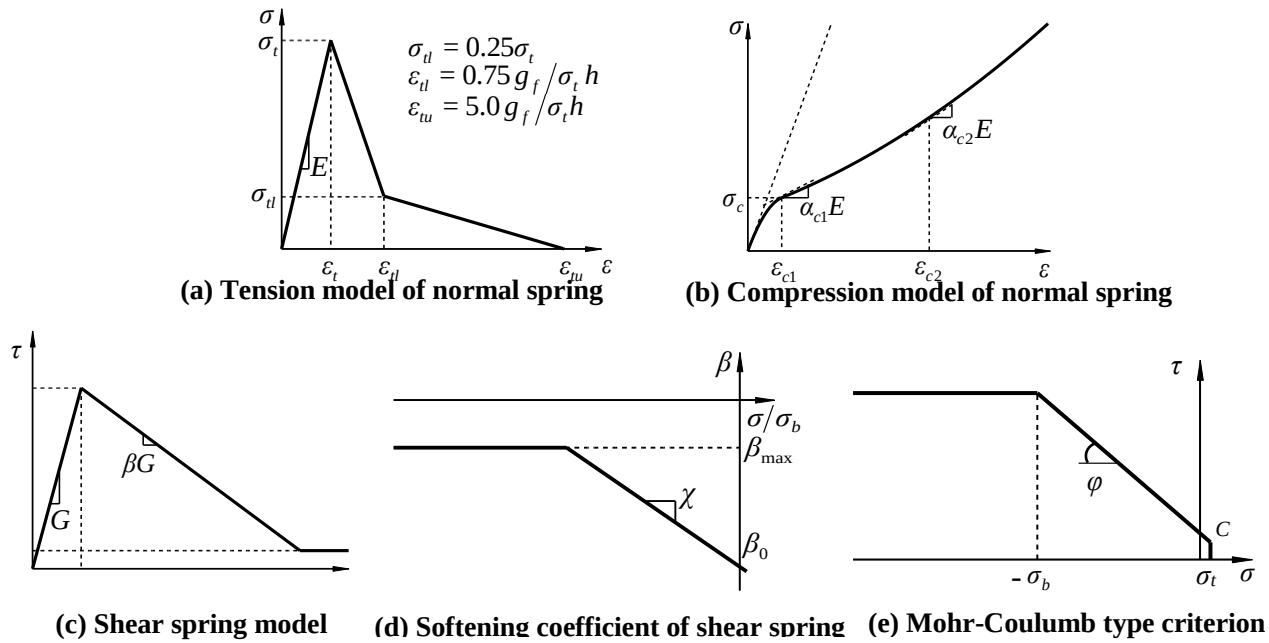

(a) Tension model of normal spring **(b) Compression model of normal spring**

(c) Shear spring model **(d) Softening coefficient of shear spring** **(e) Mohr-Coulumb type criterion**

Figure 3: Constitutive model for concrete

tensile strength, the tensile behavior of concrete is modeled as linear elastic and, after cracking, a bilinear softening branch according to 1/4 model is assumed. In the model, σ_t, g_f and h represent tensile strength, tensile fracture energy, and distance between nuclei, respectively. Figure 3b shows the stress–strain relationship for compression of normal springs that was modeled as a S-shape curve combining two quadratic functions. The parameters of σ_c, ε_{c2}, α_{c1} and α_{c2} shown in Figure 3b are material parameters which controlled the nonlinearlity of the compression behavior of the normal spring.

The shear stress–strain relationship represents the combination of two shear springs. The envelope of the stress–strain relationship for shear is given in Figure 3c. The stress elastically increases up to the shear strength with the slope of shear modulus G and softening behavior is also assumed. β is the shear-softening coefficient. It is assumed that the shear softening coefficient β depends upon the stress of the normal spring as represented in Figure 3d, where, β_0, β_{max} and χ are the parameters of dependency on the normal spring for the shear-softening coefficient. The Mohr–Coulomb criterion is assumed as the failure criteria for the shear spring (Figure 3e), where c and ϕ are cohesion and the angle of internal friction, respectively. Moreover, it is assumed that the shear stress decreases with an increase in crack width at the cracked surface, which is similar to Saito's model (Saito and Hikosaka 1999). The calibrated parameters are shown in Table 1.

Table 1: Model parameters

Normal spring							Shear spring							
Elastic modulus	Tensile response		Compressive response				Elastic modulus	Fracture criterion			Softening behavior			
E N/mm^2	σ_t N/mm^2	g_f N/mm^2	σ_c N/mm^2	ε_{c2}	α_{c1}	α_{c2}	$\eta = G/E$	c N/mm^2	φ degree	σ_b N/mm^2	β_0	β_{max}	χ	κ
1.4E*	0.8f_t*	0.5G_f*	1.5f_c'*	-0.015	0.15	0.25	0.35	0.14f_c'*	37	0.65f_c'*	-0.05	-0.02	-0.01	-0.3

* The macroscopic material parameters obtained from the concrete specimens tests

E* : Young's modulus, f_t* : Tensile strength, G_f* : Fracture energy, f_c'* : Compressive strength

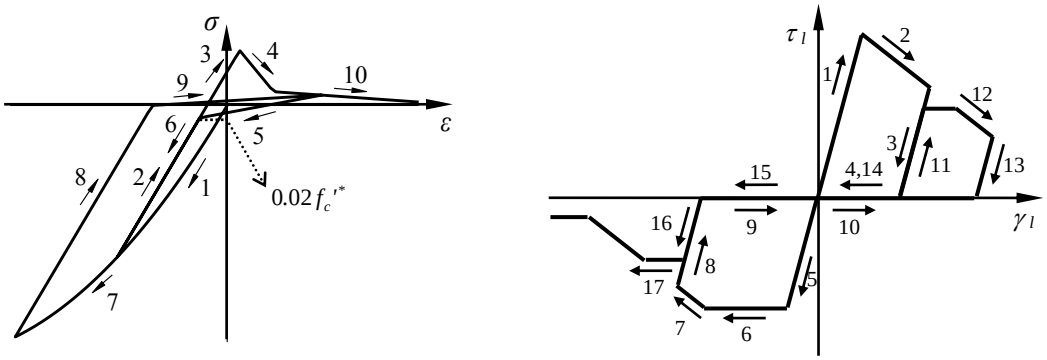

(a) Normal spring **(b) Shear spring (σ = constant)**

Figure 4: Hysteresis of stress – strain relation

Figure 4a shows the typical hysteresis loop of the normal spring (Yamamoto et al. 2013). The unloading paths in the tension zone pass toward the point of stress σ = -0.02f_c' on the compression loading path. The reloading paths in the tension zone pass toward the start point of the unloading. The stiffness of the unloading in the compression zone is initial elastic modulus *E*. Figure 4b shows the typical hysteresis loop of the shear spring. The stiffness of the unloading and reloading is initial elastic modulus *G*. In addition, after the stress reaches to zero on the unloading path, the stress keeps zero until the strain reaches to the residual strain of the opposite sign.

2.3. Reinforcement Model

Reinforcement is modeled as a series of regular beam elements (Figure 5) that can be freely located within the structure, regardless of the concrete mesh design. Three translational and three rotational degrees of freedom are defined at each beam node. The reinforcement is attached to the concrete particles by means of zero-size link elements that provide a load-transfer mechanism between the beam node and the concrete particles. For the reinforcing bar, the bilinear kinematic hardening model is applied. The hardening coefficient is 1/100. Crack development is strongly affected by the bond interaction between concrete and reinforcement. The bond stress–slip relationship is provided in the spring parallel to the reinforcement of linked element as shown in Figure 6.

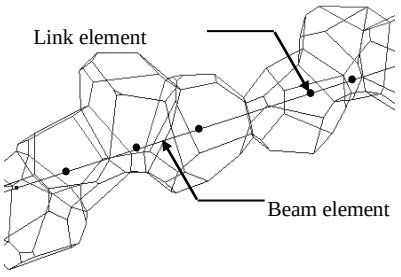

Figure 5: Reinforcement models

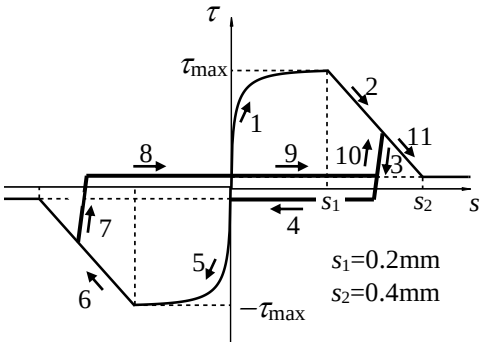

Figure 6: Bond - slip relationship

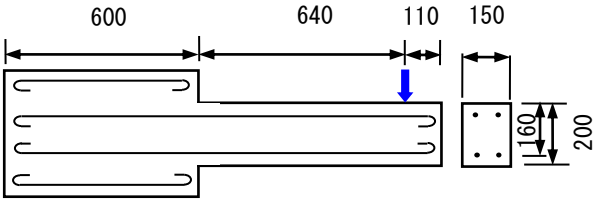

Figure 7: Dimension of specimen

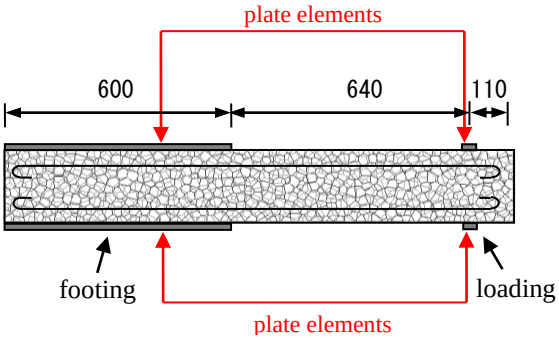

Figure 8: Analytical model

3. ANALYTICAL MODEL

The cantilever type RC beams as shown in Figure 7 is simulated. The specimen has cross section of 150×200 mm^2 and shear span of 640 mm. Two longitudinal reinforcements of D13 are arranged at upper and lower sides with cover thickness of 40 mm, and web reinforcement is not arranged. This specimen was tested by (Machida et al. 1985) and shear failure after flexural yielding under cyclic loadings were observed when displacement is 20 mm ($4\delta_y$).

Figure 8 shows analytical model which is modeled by Voronoi diagram. The average element size is about 20mm. The analysis model is modeled as a uniform cross-sectional member, and the plate element is modeled in the footing part to restrain the deformation. All reinforcements are modeled by beam element. It is assumed that compressive strength of concrete is 40.5 N/mm^2, yielding stress of longitudinal reinforcement is 380 N/mm^2.

In the analysis, displacement of loading plate element is controlled and alternative cyclic loading with incremental deformation of δ_y (5mm) is applied. Monotonic loading analysis is also conducted in order to compare with the results under cyclic loading.

4. APPLICABILITY OF 3D RBSM TO SHEAR FAILURE AFTER FLEXURAL YIELDING

Figure 9 shows load-displacement relationship obtained by analysis.The black line shows the result of cyclic loading analysis, the red line shows the result of monotonic analysis and the blue line shows the experimental results. The envelope of load displacements of cyclic and monotonic loading is almost same until $2\delta_y$ (10 mm). However, the load carrying capacity under cyclic loading decreases after $3\delta_y$. At $4\delta_y$ that shear failure occurred in the test, the load carrying capacity decreases rapidly, and the shape of hysteresis loop change to S-shape. The behavior is usually observed in the test of shear failure of RC column. The difference with the result of monotonic analysis increases according to the displacement increase.

Figure 10 and Figure 11 show deformations at 20 mm ($4\delta_y$) obtained from monotonic and cyclic loading analysis, respectively. It is understand that the flexural behavior is dominant in the monotonic loading case. On the other hand, in the cyclic loading case, diagonal crack is dominant and flexure crack does not develop. Moreover, it is observed that the deformation to lateral

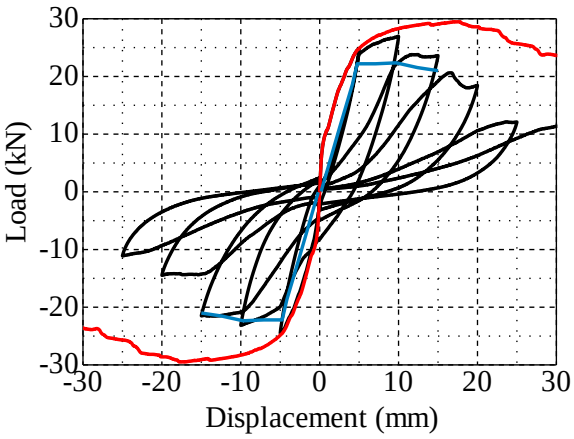

Figure 9: Load-displacement relationship

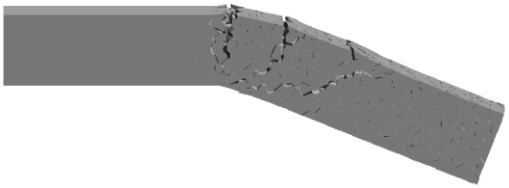

Figure 10: Deformation under monotonic loading at 20mm

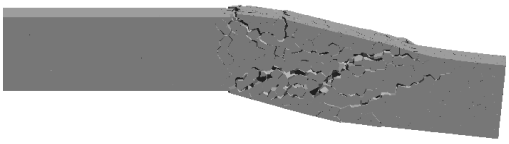

Figure 11: Deformation under cyclic loading at 20mm (4δy)

direction and X-shape crack occur. This result is clearly different from monotonic one and show typical shear failure behavior. The applicability of 3D RBSM to the shear failure after flexural yielding under cyclic loading is confirmed.

5. EVALUTION OF SHEAR STRENGTH DEGRADATION

5.1. Method to evaluate shear strength degradation

As described in introduction, the reason why the shear failure after flexural yielding occur is that the shear strength degrades under cyclic loading, although the shear strength (V_c in Figure 12) is higher than the flexural strength (P_u in Figure12) in the initial stage. Therefore, the degradation behavior of shear strength should be clarified quantatively in order to evaluate the shear failure after yielding. However, it is difficult to understand the degradation behavior in test, since the degraded shear strength in test is given by only a point on load-displacement relationship (point A in Fig.12). In order to obtain shear strength degradation behavior, an analytical method is proposed. Figure 12 shows a concept of the proposed method. The details of this method is explained following.

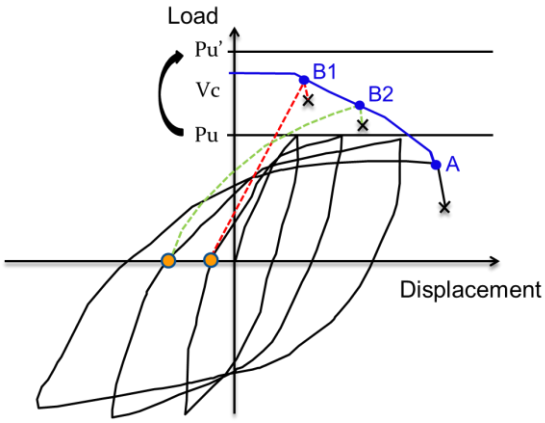

Figure 12: Concept of method

It is supposed that shear failure after yielding occur due to the degradation of shear strength as blue line in Figure12. The shear strength on the blue line such as B1 and B2 after displacement increase under cyclic loading can not be obtained, because the load does not increase over P_u which corresponds to flexural strength. However, if the flexural strength at each cycles is changed over the blue line in the analysis, the shear strength can be obtained. In order to achieve the requirement, it is proposed that the yielding stress of longitudinal reinforcement is replaced by the higher values at orange points in each cycles in Figure 12, which result in increase of flexural strength to P_u'. Then,

the shear strength in blue line less than increased flexural strength P_u' is calculation. The proposed method is based on fact that the yielding stress of longitudinal reinforcement increase only the flexural strength and does not influence to the shear strength. This method utilize the merit of numerical analysis which can consider the virtual situation.

5.2. Shear strength degradation behavior

The proposed method explained in previous chapter is applied to RC member simulated in chapter 3. The yield stress of the longitudinal reinforcement is increased from 380 to 900 N/mm^2 at each cycle, when load is 0 after unloading in negative loadings.

Figure 13 shows load-displacement relationship obtained from the proposed method. The shear strength obviously degrades with increase of displacement. The shear strength after $1\delta_y$ loading degraded little from initial strength and the strength is higher from the flexural strength. Therefore, the shear failure did not occur at the stage in the test. On the other hand, the shear strength after $3\delta_y$ degraded remarkably. Because the degraded shear strength are lower than the flexural strength in Figure 9, shear failure occur independent on increasing the yield stress of the longitudinal reinforcement.

The shear strength degradation under monotonic loading is evaluated using same method. The yield stress of longitudinal reinforcement is increased after unloading until 0 load at each displacement under monotonic loading. Figure 14 shows load-displacement relationship to obtain shear strength in after flexural yielding. The shear strength hardly degrade until $3\delta_y$ loading. The shear strength gradually decrease after $3\delta_y$ loading, and the each post peak behavior coincide. This result shows obviously different from the result under cyclic loading.

Figure 15 shows the relationship between reduction coefficient and ductility factor. The reduction

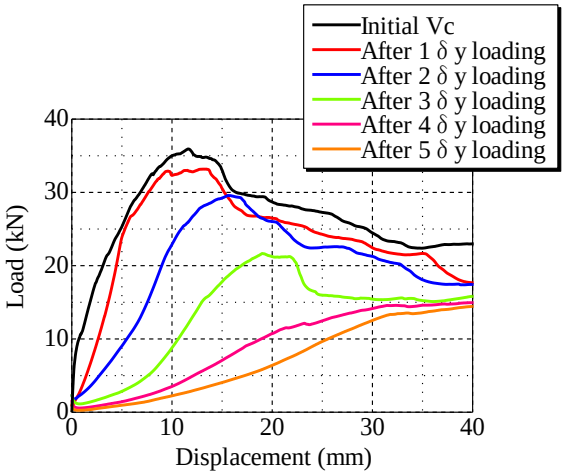

Figure 13: Load-displacement relationship

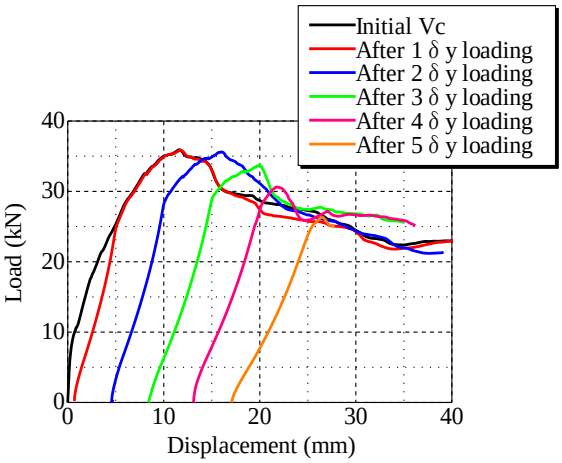

Figure 14: Load-displacement relationship

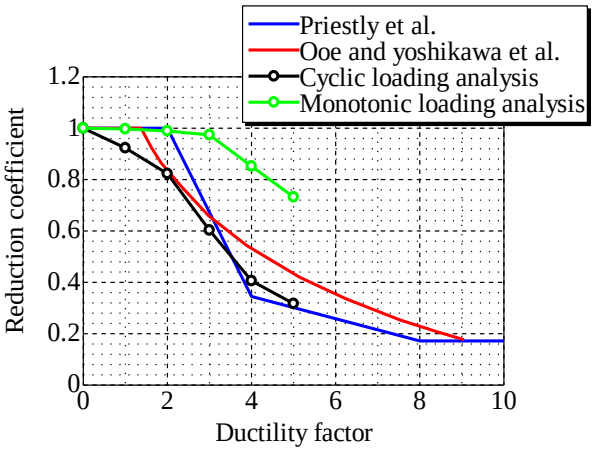

Figure 15: α-μ relationship

coefficient is defined by the ratio of shear strength at each cycle to the initial shear strength. The ductility factor is in multiples of δ_y. It was shown that the strength degradation curve obtained by cyclic loading analysis shows similar behavior with proposed formula which obtained by statistical procedure (the red and blue line in Figure 15 (Priestley et al. 1996; Ohe and Yoshikawa 2002)). Therefore, the proposed method can properly evaluated the degradation process of shear strength after flexural yielding of RC member under cyclic loading. The green line in Figure 15 is results obtained from monotonic loading analysis. Degradation behavior under monotonic loading is obviously different from behavior of cyclic loading shear strength does not decrease rapidly.

6. CONCLUSIONS

(1) 3D RBSM can simulate shear failure after flexural yielding under cyclic loading. It shows accurate crack and deformation behaviors from flexure to shear.

(2) A method to evaluate the shear strength degradation behavior directly by numerical analysis was proposed. The method utilize the merit of numerical analysis which can consider the virtual situation.

(3) Strength degradation curve obtained by analysis shows similar behavior with proposed formula which obtained by statistical procedure. Therefore, the possibility to evaluate the degraded shear strength using numerical analysis was shown.

7. ACKNOWLEDGEMENT

This study was supported by JSPS KAKENHI Grant Number 24656278.

REFERENCES

Japan Society of Civil Engineering (2012). Standard specifications for concrete structures-2012, Design.

Priestley MJN., Seible F. and Carvi GM (1996). Seimic Design of Retrofit of Bridges, A Wiley-Interscience Publication.

Ohe R., Yoshikawa H (2002). Study on shear strength degradation of single reinforced concrete columns under repeated large deformation, *Doboku Gakkai Ronbunshuu E*. V-56, No. 711, pp. 59–71.

Yasar Hanifi Gedik., Nakamura H., Yamamoto Y., Kunieda M (2011). Evaluation of Three-Dimensional Effects in Short Deep Beams using a Rigid-Body-Spring-Model, Cement and Concrete Composites, 33(9), pp. 978-991.

Yamamoto Y., Nakamura H., Kuroda I. and Furuya N (2013). Simulation of Crack Propagation in RC Shear Wall Using a 3D Rigid-Body-Spring Model with Random Geometry, FraMCoS-8.

Saito S., Hikosaka H (1999). Numerical analysis of reinforced concrete structures using spring network model. Journal of Materials, Concrete Structures and Pavements, Vol. 44, No. 627, pp. 289-303.

Machida A., Mutsuyoshi H. and Toyoda K (1985). Evaluation of the ductility of reinforced concrete members, Annual Journal of Japan Concrete Institute, Vol. 7, No. 1, pp. 629-632.